EVALUATION MODEL OF THE STEADY-STATE HEAT TRANSFER PERFORMANCE OF TWO-PHASE CLOSED THERMOSYPHONS

by

Yafeng WU[a,b], Zhe ZHANG[b], Wenbin LI[b*], and Daochun XU[b]

[a] Key Laboratory of Particle Acceleration Physics and Technology, Institute of High Energy Physics, Chinese Academy of Sciences, Beijing, China
[b] Key Laboratory of State Forestry and Grassland Administration on Forestry Equipment and Automation, School of Technology, Beijing Forestry University, Beijing, China

Original scientific paper
https://doi.org/10.2298/TSCI200825166W

Two-phase closed thermosyphons have good thermal conductivity and are widely used in heat transfer applications. It is essential to establish an effective method for evaluating the steady-state heat transfer performance of two-phase closed thermosyphons, as such a method can help to select appropriate designs and to improve the efficiency of these devices. In this paper, the equivalent thermal conductivity is derived by the principle of equal total thermal resistance, in which the influence of the adiabatic length is eliminated. An evaluation model of the steady-state heat transfer performance of two-phase closed thermosyphons is established. Test results of three two-phase closed thermosyphons with total lengths of 220 mm, 320 mm, and 500 mm show that as the heat transfer rate increases, the equivalent thermal conductivity of these devices decreases by 28.91%, increases by 6.10% and increases by 10.02%, respectively, among which the minimum value is 831.63 W/mK and the maximum value is 1694.19 W/mK. The decrease (increase) in the equivalent thermal conductivity in the evaluation model indicates a decrease (increase) in the heat transfer performance. The results show that the equivalent thermal conductivity of the model can effectively evaluate the heat transfer performance of two-phase closed thermosyphons.

Key words: *two-phase closed thermosyphon, heat transfer performance, evaluation model, equivalent thermal conductivity*

Introduction

A two-phase closed thermosyphon, also known simply as a thermosyphon, is a kind of heat transfer element with a high heat transfer efficiency [1]. These devices have the advantages of simple structures, low manufacturing costs and excellent heat transfer performance [2]. A two-phase closed thermosyphon has high reliability, high efficiency, low cost, and no wick, moreover, two-phase closed thermosyphons are easier to manufacture than other types of thermosyphons [3]. A thermosyphon is generally composed of a metal tube and a working fluid. The manufacturing process of a thermosyphon involves pulling a vacuum on the metal tube, filling the tube with the working fluid, and then sealing the thermosyphon. A schematic diagram of the working principle of a two-phase closed thermosyphon is shown in fig. 1. A thermosy-

* Corresponding author, e-mail: leewb@bjfu.edu.cn

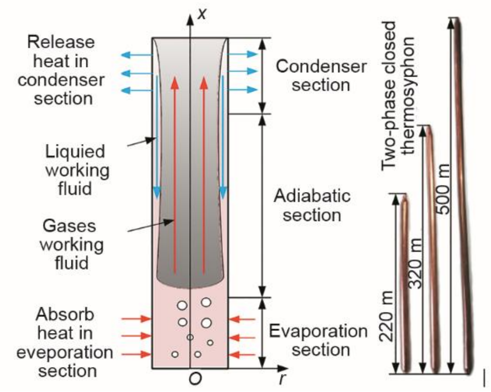

Figure 1. Schematic diagram of the working principle of a two-phase closed thermosyphon

phon can be divided into three parts: the evaporation section, the adiabatic section, and the condensation section. The phase change heat transfer process of a thermosyphon under normal operation is as follows. The heat absorbed by the evaporation section causes the liquid working fluid to change phase (*i.e.*, form liquid to gas); the energy is stored as latent heat. The gaseous working fluid moves to the condensation section, wherein the latent heat is released and the working fluid change phase (*i.e.*, form gas to liquid). Finally, gravity drives the liquid working fluid back to the evaporation section [4]. The thermosyphon has the advantages of a simple structure, stable operation and a wide working temperature range, thus, thermosyphons are widely used in industrial fields [5]. The effective evaluation of the steady-state heat transfer performance of a two-phase closed thermosyphon can guide its design under different working conditions, which is of great significance for improving heat transfer efficiency in engineering applications.

At present, research on thermosyphons is generally based on the theory of heat transfer, simulations with relevant software, and experimental measurements of heat transfer performance. Kafeel and Turan [6] studied the heat transfer characteristics of a thermosyphon under different pulsed heat increments, moreover, they simulated the evaporation and condensation process of a thermosyphon with the Eulerian model, considering the effects of evaporation, condensation, heat transfer and mass transfer at the interface in the two-phase region. Wang *et al.* [7] used the modified Lee model based on the volume of fluid method and the original Lee model to model the heat transfer behavior of a thermosyphon during geyser boiling via CFD. Ma *et al.* [8] established a transient simulation model of a thermosyphon using SINDA/FLUINT 5.6. The evaporation section was heated with a water bath and the heat transfer rate and the total heat transfer coefficient increased with increasing water bath temperature.

Aghel *et al.* [9] studied the heat transfer performance of a new condenser of a two-phase closed thermosyphon that utilized distilled water as the working fluid. The wall temperature difference between the evaporation section and the condensation section of the thermosyphon with the new condenser was smaller than that of the ordinary thermosyphon. Payakaruk *et al.* [10] studied the heat transfer characteristics of a two-phase closed thermosyphon filled with water, ethanol, R22, R123, and R134a at different inclination angles, filling rates and input powers. The position-specific heat transfer ratio is the heat transfer rate when the thermosyphon is placed at any angle compared with the heat transfer rate when the thermosyphon is placed at a vertical angle. The position-specific heat transfer ratio is not affected by the filling ratio but by the thermophysical properties of the working fluid. Esen and Esen [11] studied the influence of different working fluids on the thermal performance of a two-phase closed thermosyphon solar collector. In their study, they investigated the performance of the device under sunny conditions and presented the detailed temperature distribution and the energy collection efficiency. Jiao *et al.* [12] established a comprehensive model to study the effects of heat input, working pressure, geometry and liquid filling ratio on the heat transfer performance of a vertical thermosyphon. They obtained a combined correlation for the heat transfer rate of the evaporation section based on the effective area, and they found that this correlation is superior to other heat transfer correlations. Sukchana and Jaiboonma [13] carried out experiments on a straight copper tube thermosyphon with R-134a as the working fluid to study the influence of the working fluid filling ratio and the adiabatic section length on the heat transfer efficiency of the thermosyphon and subsequently determined the optimal working conditions. Noie *et al.* [14] conducted an experimental study on the thermal performance of a two-phase closed thermosyphon with different liquid filling rates under normal working conditions and found that when the working fluid filling ratio was greater than 30%, geyser boiling will occur, although this phenomenon does not limit the heat transfer performance of the thermosyphon, it will damage the condensation section due to blockages or impacts. Jafari *et al.* [15] conducted numerical simulations and experimental research on a two-phase closed thermosyphon and found that, under the conditions of normal operation, the numerical predictions for the maximum heat transfer rate caused by transient local dryout were basically consistent with the experimental results.

In recent years, research on nanofluids has received increasing attention, thus, nanofluids have been used to replace some conventional working fluids [16-18]. Naphon *et al.* [19] enhanced the heat transfer characteristics of a heat transfer device by changing the flow characteristics of the working fluid and proposed a method for improving the efficiency of a heat pipe by using nanofluids. Khandekar *et al.* [20] studied the overall thermal resistance of two-phase closed thermosyphons that utilized pure water and various water-based nanofluids as working fluids. The thermal performance of these nanofluids was not as good as that of pure water. The wettability of the nanoparticles in the grooves of surface roughness results in poor thermal performance. Yu *et al.* [21] carried out a numerical simulation of the transient natural convection heat transfer of water-based nanofluids in a horizontal ring of a coaxial cylinder. When the Rayleigh number was constant, the Nusselt number gradually decreased as the volume fraction of the nanoparticles increased.

The heat transfer performance of two-phase closed thermosyphons has been studied by many methods in the existing literature. The temperature difference between the evaporation section and the condensation section of a two-phase closed thermosyphon is often used to indicate the heat transfer performance of a thermosyphon, whereas an evaluation index of heat transfer performance during steady-state operation is not given. In this paper, a heat transfer evaluation model of a two-phase closed thermosyphon is established, wherein the equivalent thermal conductivity is derived by the principle of equal total thermal resistance, and the influence of the adiabatic section length on the model is eliminated. The experimental results show that the evaluation model can effectively assess the heat transfer performance of a thermosyphon during steady-state operation, which is of great significance for engineering applications of two-phase closed thermosyphons.

Theory

According to the theory of heat transfer, the total thermal resistance, R, of a two-phase closed thermosyphon can be expressed:

$$R=\frac{\ln\dfrac{d_o}{d_i}}{2\pi\lambda_w L_e}+\frac{1}{h_e\pi d_i L_e}+\frac{1}{h_c\pi d_i L_c}+\frac{\ln\dfrac{d_o}{d_i}}{2\pi\lambda_w L_c} \tag{1}$$

where d_o, d_i, L_e, and L_c are the outer diameter, inner diameter, evaporation section length, and condensation section length of the thermosyphon, respectively, λ_w – the thermal conductivity of the tube wall material, and h_e and h_c – the convective heat transfer coefficients of the evaporation section and the condensation section, respectively. The four thermal resistance terms on the right side of eq. (1) can be divided into two categories: the first and fourth terms are the thermal resistance, R_w, of the wall of the thermosyphon, and the second and third terms are the thermal resistance, R_v, of the phase change heat transfer of the working fluid inside the thermosyphon.

$$R_w = \frac{\ln\dfrac{d_o}{d_i}}{2\pi\lambda_w L_e} + \frac{\ln\dfrac{d_o}{d_i}}{2\pi\lambda_w L_c} \tag{2}$$

$$R_v = \frac{1}{h_e \pi d_i L_e} + \frac{1}{h_c \pi d_i L_c} \tag{3}$$

The heat transfer resistance in a thermosyphon is mainly composed of convective heat transfer accompanied by the phase transformation between the evaporation section and the condensation section. The saturation temperature drop caused by the pressure drop of the steam flow from the evaporation section to the condensation section is equivalent to the existence of a negligible thermal resistance value, Bashir *et al.* [22]. The equivalent length, L_{eff}, is defined, which can simultaneously characterize the lengths of the evaporation section and the condensation section:

$$L_{eff} = L_e + L_c \tag{4}$$

The heat transfer process in a thermosyphon is convective heat transfer with phase change. The factors that affect this heat transfer process are very complex. It is difficult to obtain the specific values of h_e and h_c through a theoretical analysis. Suppose that the thermal conductivity of a cylinder is the equivalent thermal conductivity, $\lambda_{eff,v}$, of the working fluid, the length is the equivalent length, L_{eff}, the cross-sectional area is the same as that of the vapor space, A_v, and the equivalent thermal resistance is the same as that of the phase change heat transfer of the working fluid, R_v, which can be expressed:

$$R_v = \frac{L_{eff}}{\lambda_{eff,v} A_v} \tag{5}$$

According to eqs. (3) and (5), the expression of $\lambda_{eff,v}$ can be obtained:

$$\lambda_{eff,v} = \frac{4L_{eff}}{d_i\left[\dfrac{1}{h_e L_e} + \dfrac{1}{h_c L_c}\right]} \tag{6}$$

where $\lambda_{eff,v}$ simultaneously takes into account the influence of the length of the evaporation section, L_e, the length of the condensation section, L_c, and the convective heat transfer coefficients, h_e and h_c, on the heat transfer performance of the thermosyphon, while excluding the influence of the length of the adiabatic section. The total thermal resistance of the thermosyphon is calculated:

$$R = \frac{T_e - T_c}{Q} = \frac{\Delta T}{Q} \tag{7}$$

where T_e and T_c are the average temperatures of the outer wall of the evaporation section and the condensation section, respectively, and Q – the heat transfer rate of the thermosyphon.

According to eqs. (1), (2), (5), and (7), the formula for calculating the value of $\lambda_{\mathrm{eff},v}$ is expressed:

$$\lambda_{\mathrm{eff},v} = \frac{L_{\mathrm{eff}}}{A_v \dfrac{T_\mathrm{e} - T_\mathrm{c}}{Q - R_\mathrm{w}}} \tag{8}$$

where R_w term in the heat transfer resistance of the thermosyphon is equivalent to the same cylinder size in eq. (5). According to eq. (2), the equivalent thermal conductivity $\lambda_{\mathrm{eff,w}}$ of the tube wall is:

$$\lambda_{\mathrm{eff},w} = \frac{8L_\mathrm{e}L_\mathrm{c}\lambda_\mathrm{w}}{d_\mathrm{i}^2 \ln \dfrac{d_\mathrm{o}}{d_\mathrm{i}}} \tag{9}$$

According to eqs. (1), (5), and (9), the equivalent model of the total thermal resistance of the thermosyphon can be obtained:

$$R = \frac{L_{\mathrm{eff}}}{A_v}\left(\frac{1}{\lambda_{\mathrm{eff},v}} + \frac{1}{\lambda_{\mathrm{eff,w}}}\right) \tag{10}$$

In the evaluation model, the total equivalent thermal conductivity λ_{eff} of the two--phase closed thermosyphon is a parameter used to evaluate its steady-state heat transfer performance, and the corresponding relationship with $\lambda_{\mathrm{eff},v}$ and $\lambda_{\mathrm{eff,w}}$ is:

$$\frac{1}{\lambda_{\mathrm{eff}}} = \frac{1}{\lambda_{\mathrm{eff},v}} + \frac{1}{\lambda_{\mathrm{eff,w}}} \tag{11}$$

Experiments

A schematic of the experimental device is shown in fig. 2. The whole experimental system is divided into four parts: the heat pipe part, the heating part, the cooling part, and the temperature acquisition part. Three cylindrical copper two-phase closed thermosyphons with ethanol as the working fluid and total lengths of 220 mm, 320 mm, and 500 mm are used in the experiment and the specific parameters are given in tab 1. The volume of the working fluid varies, while the filling ratio stays the same. The filling ratio represents the ratio of working fluid volume to inner volume of the thermosyphon. The heating part consists of an electronic voltage regulator module, a PF9901 power meter, a heating rod and a copper heating block. The cooling part is composed of a cooling circulating pump, a copper cooling block, a water-cooled cooling plate and a water tank. The temperature measurement part is composed of a *T*-type thermocouple and an MIK-R4000D acquisition instrument. During the experiment, the heating rod was powered by the electronic voltage regulator module with 220 VAC-50 Hz, the heating power was controlled by the voltage regulating knob, and the heating power was determined by the PF9901 power meter. Two heating rods and the evaporation section of the thermosyphon are inserted into the copper heating block, and the heat generated by the heating rod is indirectly transmitted to the heat pipe through the heating block. This approach provides uniform heating to the evaporation section of the thermosyphon. The thermosyphon is oriented vertically, the condensation section is inserted into the copper cooling block, and the water-cooled cooling plates are fixed on both sides of the cooling block. The circulating pump drives the coolant to dissipate the heat released from the condensation section.

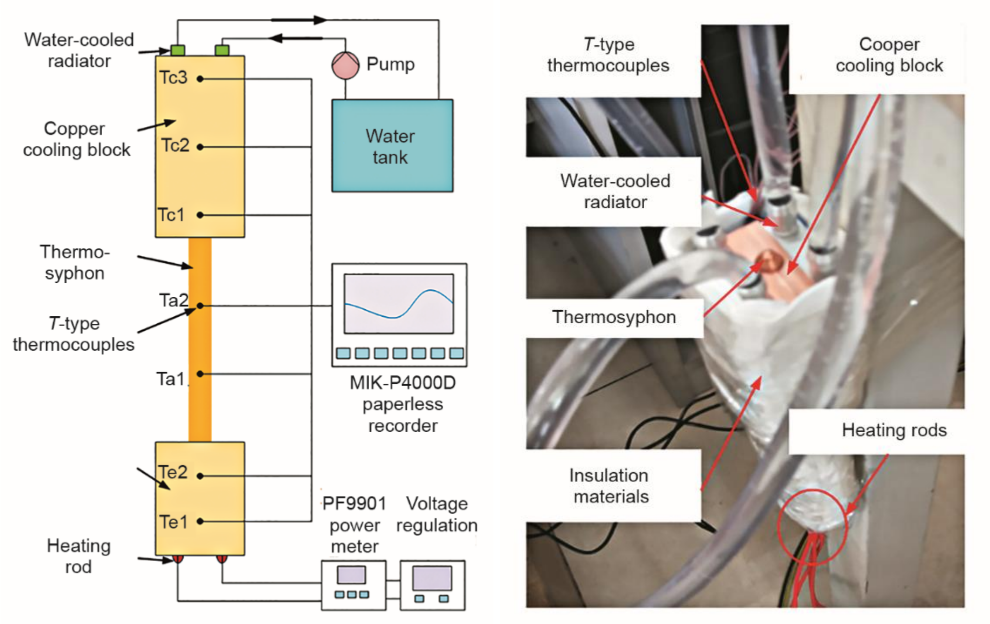

Figure 2. Schematic of the experimental set-up

Table 1. Experimental parameters of the thermosyphon

Parameter	Value
Body material	Copper
Working fluid	Ethanol
Length [mm]	220/320/500
Evaporation length [mm]	50/50/50
Adiabatic length [mm]	90/190/370
Condenser length [mm]	80/80/80
Inner diameter [mm]	7.6
Outer diameter [mm]	10
Filling ratio [%]	22.7

Seven *T*-type thermocouples are arranged outside the wall of the thermosyphon for temperature measurements. The distance from the bottom of the thermosyphon is given in tab. 2. Thermocouples Te1 and Te2 are in the evaporation section, thermocouples Ta1 and Ta2 are in the adiabatic section, and thermocouples Tc1, Tc2, and Tc3 are in the condensation section. To reduce the heat loss during the heat transfer process of the thermosyphon and to minimize the impact of the external environment, the thermosyphon, heating block, cooling block and water-cooled heat sink are wrapped with ceramic fiber paper insulation material. Heat insulation treatment can reduce the heat loss of the system to the environment, and the heat loss rate can be less than 10% [23].

Table 2. Distance between the *T*-type thermocouples and the bottom of the thermosyphon

Distance [mm]	Te1	Te2	Ta1	Ta2	Tc1	Tc2	Tc3
L = 220	15	35	80	110	150	180	210
L = 320	15	35	110	180	250	280	310
L = 500	15	35	170	290	430	460	490

This experiment was divided into three groups. Two-phase closed thermosyphons with total lengths of 220 mm, 320 mm, and 500 mm were tested for heat transfer performance. The heating powers tested were 20-60 W. To calculate the uncertainty of the whole experiment, the theory introduced in reference [24] is used. The uncertainty of the instrument used in the experiment is governed by the AC frequency accuracy (±0.1%), the power meter accuracy (±0.5%), and the T-type thermocouple accuracy (±0.5 °C).

Results and discussion

The temperature gradients under steady-state conditions of the three two-phase closed thermosyphons with different lengths are shown in fig. 3. The three diagrams in fig. 3 show that the temperature of each point increases with increasing heat transfer rate, and the temperature gradients of the different heat transfer rates are similar, which is consistent with the results reported in the literature [25]. When the heat transfer rate is 60 W, the maximum temperature differences between the evaporation section and the condensation section were 206.75 K, 124.97 K, and 101.49 K for total thermosyphon lengths of 220 mm, 320 mm, and 500 mm, respectively. According to fig 3(b), the temperature in the evaporation section of the two-phase closed thermosyphon with a total length of 320 mm tends to increase. This phenomenon occurs due to stable film boiling in the middle of the evaporation section, which leads to a high temperature there. This high temperature will reduce the heat transfer. When

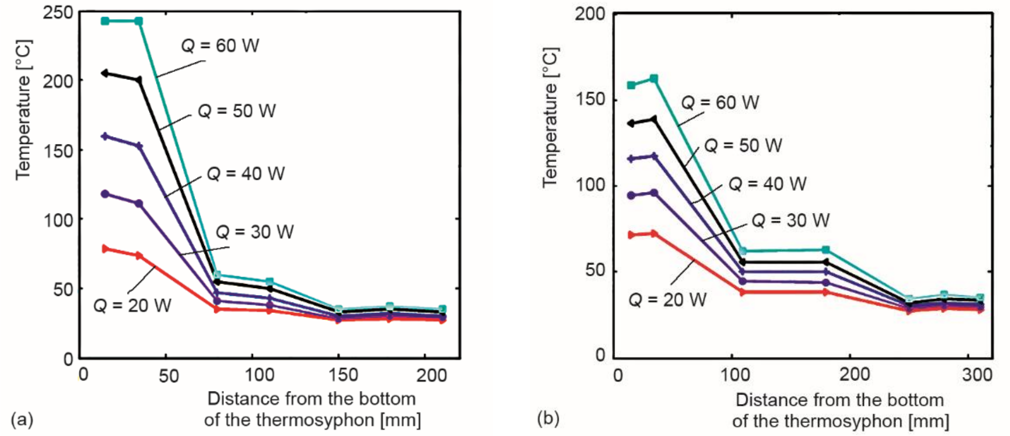

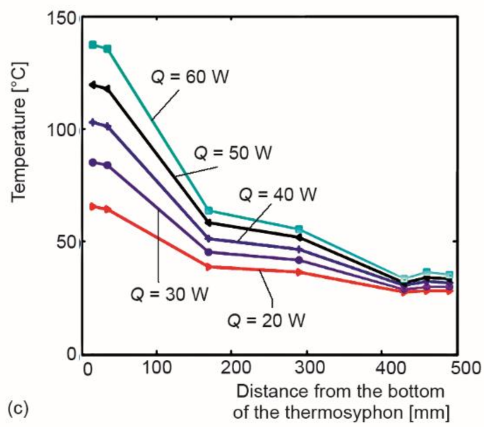

Figure 3. Temperature gradient on the outer wall of the two-phase closed thermosyphon at different heat transfer rates; (a) L = 220 mm, (b) L = 320 mm, and (c) L = 500 mm

the heat transfer rate is 60 W, the two-phase closed thermosyphon with a total length of 220 mm also shows a similar situation. A comparison of three diagrams in fig. 3 shows that the evaporation section of the two-phase closed thermosyphon with a total length of 220 mm has the highest temperature at the same heat transfer rate, which indicates that its heat transfer performance is worse than those of the other two. This thermosyphon has the worst performance because it contains less working fluid than the other two thermosyphons; thus, increasing the heat transfer rate makes the working fluid unable to return in time. Figure 3(c) shows that the two-phase closed thermosyphon with a total length of 500 mm has the best heat transfer performance. This thermosyphon has the best performance because it contains the most working fluid. Hence, for this thermosyphon, when the heat transfer rate is higher, there is sufficient reflux liquid working fluid and after the endothermic phase change, the working fluid carries heat to the condensation section. Therefore, the thermosyphon with a total length of 500 mm has the strongest heat transfer capacity among the three thermosyphons evaluated herein.

According to the temperature measurements, the difference between the average temperatures of the evaporation section and the condensation section of the two-phase closed thermosyphon and the total thermal resistance value are calculated. The results are shown in figs. 4(a) and 4(b). As heat transfer rate increased, the temperature difference at both ends of the two-phase closed thermosyphon increased, and the temperature difference of the two-phase closed thermosyphon with a total length of 220 mm was obviously higher than that of the other two thermosyphons. However, the three thermosyphons do not exhibit the same trends in terms of the total thermal resistance.

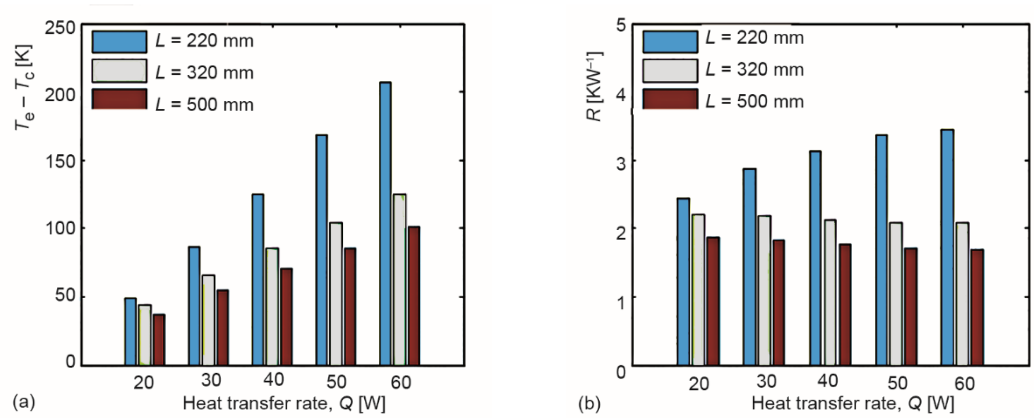

Figure 4. Effect of the heat transfer rate on; (a) the average temperature difference in the evaporation section and the condenser section and (b) the total thermal resistance

The two-phase closed thermosyphon with a total length of 220 mm increases with increasing heat transfer rate. However, the total thermal resistance of the other two thermosyphons decreases with increasing heat transfer rate, and the heat transferred per unit temperature difference increases, hence, the heat transfer performance of the thermosyphon increases. When there is a sufficient amount of liquid in the thermosyphon, increasing the heat transfer rate will increase the evaporation capacity of the liquid working fluid and then lead to an increase in temperature. However, there is enough liquid working fluid reflux to supplement, thus, the total thermal resistance exhibits a downward trend and the heat transfer performance increases. This finding is consistent with the results reported in [14].

The relationship between the total equivalent thermal conductivity, λ_{eff}, and the heat transfer rate of the three two-phase closed thermosyphons is shown in fig. 5. The total equivalent thermal conductivity in the evaluation model of the two-phase closed thermosyphon changes with increasing heat transfer rate. The total equivalent thermal conductivity of the two-phase closed thermosyphon with a total length of 220 mm decreases and with increasing heat transfer rate. When the heat transfer rate is 20 W, the equivalent thermal conductivity is 1169.84 W/mK. When the heat transfer rate is increased to 60 W, the equivalent thermal conductivity is 831.63 W/mK, which is a 28.91% decrease and this finding shows that the heat transfer performance is decreasing. The reason this phenomenon occurs is that, with the increase in input power, the evaporation rate of the working fluid in the evaporation section of the two-phase closed thermosyphon increases, and the working fluid cannot be added back in time, thereby decreasing the heat transfer performance. The equivalent thermal conductivity of the two-phase closed thermosyphons with total lengths of 320 mm and 500 mm increases with increasing heat transfer rate, which is consistent with the results reported in [8, 26]. The equivalent thermal conductivity of the former increased from 1296.69 W/mK to 1375.84 W/mK (a 6.10% increase), whereas that of the latter increased from 1539.88 W/mK to 1694.19 W/mK (a 10.02% increase). Hence, the heat transfer performance of both of these thermosyphons has been improved. This phenomenon occurs because the increase in the heat transfer rate can accelerate the boiling of the working fluid in the evaporation section, and the reflux rate of the working fluid can meet the requirements of evaporation.

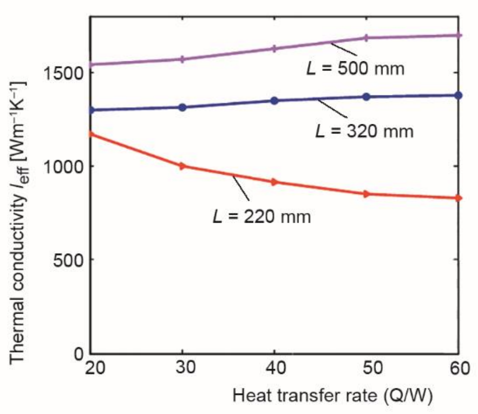

Figure 5. Relationship between total equivalent thermal conductivity and heat transfer rate

The decrease (increase) in the total equivalent thermal conductivity in the evaluation model indicates a decrease (increase) in the heat transfer performance of the two-phase closed thermosyphon. A comparison of the results in figs. 4(a), 4(b), and (5) show that the evaluation model can represent the steady-state heat transfer performance of a two-phase closed thermosyphon.

Conclusions

Based on the principle of the equal total thermal resistance, the equivalent thermal conductivity of the two-phase closed thermosyphon is derived, and an evaluation model of the steady-state heat transfer performance of the two-phase closed thermosyphon is obtained. The validity of the evaluation model is verified by an experimental study of three two-phase closed thermosyphons with different total lengths.

- The total equivalent thermal conductivity of the two-phase closed thermosyphon with a total length of 220 mm decreases with an increasing heat transfer rate. When the heat transfer rate increases from 20-60 W, the equivalent thermal conductivity of this thermosyphon decreases by 28.91%. When the heat transfer rate increases from 20-60 W, the equivalent thermal conductivities of the two-phase closed thermosyphons with total lengths of 320 mm and 500 mm increase by 6.10% and 10.02%, respectively. The experimental results show that the evaluation model can effectively evaluate the steady-state heat transfer performance of a two-phase closed thermosyphon.

- This evaluation model excludes the influence of the length of the adiabatic section on the equivalent thermal conductivity, and the steady-state heat transfer performances of two-phase closed thermosyphons of different sizes can be compared. When the heat transfer rates are 20-60 W, the equivalent heat transfer coefficients of the two-phase closed thermosyphon with a total length of 500 mm are 1539.88 W/mK, 1566.43 W/mK, 1624.19 W/mK, 1680.63 W/mK and 1694.19 W/mK, respectively, which shows that the equivalent heat transfer coefficients are higher than the other two thermosyphons at any heat transfer rate; hence, this thermosyphon has better heat transfer performance than the other two thermosyphons.

Acknowledgment

The financial support from the National Science Foundation of China (31670716), the China Postdoctoral Science Special Foundation (2016T90044) and the China Postdoctoral Science Foundation (2015M570945) is gratefully acknowledged.

Nomenclature

A_v – cross-sectional area of the vapor space, [m^2]
d_i – inner diameter, [m]
d_o – outer diameter, [m]
h_e – convective heat transfer coefficient of evaporation, [$Wm^{-1}K^{-1}$]
h_c – convective heat transfer coefficient of condensation, [$Wm^{-1}K^{-1}$]
L – total length of the two-phase closed thermosyphon, [m]
L_e – length of the evaporation section, [m]
L_a – length of the adiabatic section, [m]
L_c – length of the condensation section, [m]
L_{eff} – equivalent length of the two-phase closed thermosyphon, [m]
T_e – average temperature of the evaporation section, [°C]
T_c – average temperature of the condensation section, [°C]
Q – heat transfer rate, [W]
R – total thermal resistance of the thermosyphon, [KW^{-1}]
R_w – wall heat conduction resistance, [KW^{-1}]
R_v – thermal resistance of the phase change heat transfer, (KW^{-1})

Greek symbols

λ_{eff} – total equivalent thermal conductivity, [$Wm^{-1}K^{-1}$]
$\lambda_{eff,v}$ – equivalent thermal conductivity of the working fluid, [$Wm^{-1}K^{-1}$]
$\lambda_{eff,w}$ – equivalent thermal conductivity of the tube wall, [$Wm^{-1}K^{-1}$]
λ_w – thermal conductivity of the tube wall materials, [$Wm^{-1}K^{-1}$]

References

[1] Noie, S. H., *et al.,* Heat Transfer Enhancement Using Al_2O_3/Water Nanofluid in a Two-Phase Closed Thermosyphon, *International Journal of Heat and Fluid Flow, 30* (2009), 4, pp. 700-705
[2] Noie, S. H., Heat transfer Characteristics of a Two-Phase Closed Thermosyphon, *Applied Thermal Engineering, 25* (2005), 4, pp. 495-506
[3] Zhang, H., Zhuang, J., Research, Development and Industrial Application of Heat Pipe Technology in China, *Applied Thermal Engineering, 23* (2003), 9, pp. 1067-1083
[4] Fadhl, B., *et al.,* Numerical Modelling of the Temperature Distribution in a Two-Phase Closed Thermosyphon, *Applied Thermal Engineering, 60* (2013), 1-2, pp. 122-131
[5] Jafari, D., *et al.,* An Experimental Investigation on the Evaporation and Condensation Heat Transfer of Two-Phase Closed Thermosyphons, *Experimental Thermal and Fluid Science, 88* (2017), Nov., pp. 111-123

[6] Kafeel, K., Turan, A., Simulation of the Response of a Thermosyphon Under Pulsed Heat Input Conditions, *International Journal of Thermal Sciences, 80* (2014), June, pp. 33-40
[7] Wang, X., *et al.,* A Combined CFD/Visualization Investigation of Heat Transfer Behaviors During Geyser Boiling in Two-Phase Closed Thermosyphon, *International Journal of Heat and Mass Transfer, 121* (2018), June, pp. 703-714
[8] Ma, L., *et al.,* Modelling of Two-Phase Closed Thermosyphon Based on SINDA/FLUINT, *Applied Thermal Engineering*, *130* (2018), Feb., pp. 375-383
[9] Aghel, B., *et al.,* Heat-Transfer Enhancement of Two-Phase Closed Thermosyphon Using a Novel Cross-Flow Condenser, *Heat and Mass Transfer, 53* (2016), 3, pp. 765-773
[10] Payakaruk, T., *et al.,* Correlations to Predict Heat Transfer Characteristics of an Inclined Closed Two-Phase Thermosyphon at Normal Operating Conditions, *Applied Thermal Engineering, 20* (2000), 9, pp. 781-790
[11] Esen, M., Esen, H., Experimental Investigation of a Two-Phase Closed Thermosyphon Solar Water Heater, *Solar Energy*, *79* (2005), 5, pp. 459-468
[12] Jiao, B., *et al.,* Investigation on the Effect of Filling Ratio on the Steady-State Heat Transfer Performance of a Vertical Two-Phase Closed Thermosyphon, *Applied Thermal Engineering, 28* (2008), 11-12, pp. 1417-1426
[13] Sukchana, T., Jaiboonma, C., Effect of Filling Ratios and Adiabatic Length on Thermal Efficiency of Long Heat Pipe Filled with R-134a, *Energy Procedia, 34* (2013), Dec., pp. 298-306
[14] Noie, S. H., *et al.,* Effect of Inclination Angle and Filling Ratio on Thermal Performance of a Two-Phase Closed Thermosyphon under Normal Operating Conditions, *Heat Transfer Engineering, 28* (2007), 4, pp. 365-371
[15] Jafari, D., *et al.,* Unsteady Experimental and Numerical Analysis of a Two-Phase Closed Thermosyphon at Different Filling Ratios, *Experimental Thermal and Fluid Science, 81* (2017), Feb., pp. 164-174
[16] Huminic, G., *et al.,* Experimental Study of the Thermal Performance of Thermosyphon Heat Pipe Using Iron Oxide Nanoparticles, *International Journal of Heat and Mass Transfer, 54* (2011), 1-3, pp. 656-661
[17] Sarafraz, M. M., Hormozi, F., Experimental stUdy on the Thermal Performance and Efficiency of a Copper Made Thermosyphon Heat Pipe Charged with Alumina-Glycol Based Nanofluids, *Powder Technology, 266* (2014), Nov., pp. 378-387
[18] Sarafraz, M. M., *et al.,* Thermal Performance and Efficiency of a Thermosyphon Heat Pipe Working with a Biologically Ecofriendly Nanofluid, *International Communications in Heat and Mass Transfer, 57* (2014), Oct., pp. 297-303
[19] Naphon, P., *et al.,* Experimental Investigation of Titanium Nanofluids on the Heat Pipe Thermal Efficiency, *International Communications in Heat and Mass Transfer, 35* (2008), 10, pp. 1316-1319
[20] Khandekar, S., *et al.,* Thermal Performance of Closed Two-Phase Thermosyphon Using Nanofluids, *International Journal of Thermal Sciences, 47* (2008), 6, pp. 659-667
[21] Yu, Z. T., *et al.,* A Numerical Investigation of Transient Natural Convection Heat Transfer of Aqueous Nanofluids in a Horizontal Concentric Annulus, *International Journal of Heat and Mass Transfer, 55* (2012), 4, pp. 1141-1148
[22] Bashir, A. I., *et al.,* Single-Phase Forced Convection Heat Transfer and Pressure Drop in Circular Tubes in the Laminar and Transitional Flow Regimes, *Experimental Thermal and Fluid Science, 109* (2019), Dec., 109891
[23] Sarafraz, M. M., *et al.,* Role of Nanofluid Fouling on Thermal Performance of a Thermosyphon: Are Nanofluids Reliable Working Fluid, *Applied Thermal Engineering, 82* (2015), May, pp. 212-224
[24] Moffat, R. J., Describing the Uncertainties in Experimental Results, *Experimental Thermal and Fluid Science, 1* (1988), 1, pp. 3-17
[25] Arya, A., *et al.,* Thermal Performance Analysis of a Flat Heat Pipe Working with Carbon Nanotube-Water Nanofluid for Cooling of a High Heat Flux Heater, *Heat and Mass Transfer, 54* (2017), 4, pp. 985-997
[26] Sarafraz, M. M., *et al.,* Assessment of the Thermal Performance of a Thermosyphon Heat Pipe Using Zirconia-Acetone Nanofluids, *Renewable Energy, 136* (2019), June, pp. 884-895

Paper submitted: August 25, 2020
Paper revised: April 6, 2021
Paper accepted: April 9, 2021